

Ultrasonic wave propagation and barrier-limited heat flow in thin films of $\text{YBa}_2\text{Cu}_3\text{O}_{7-x}$

C. D. Marshall, I. M. Fishman,* and M. D. Fayer

Department of Chemistry, Stanford University, Stanford, California 94305

(Received 12 October 1990)

Direct generation and detection of acoustic waveguide modes in thin ($< 1000 \text{ \AA}$) films using the optical-transient-grating method are reported. The upper limit of acoustic damping in $\text{YBa}_2\text{Cu}_3\text{O}_{7-x}$ films was measured to be $\sim 100 \text{ dB/cm}$ for 1-GHz acoustic waves at room temperature. The presence of barrier-limited thermal conductivity into the supporting MgO substrate is demonstrated and a thermal diffusivity of $0.023 \text{ cm}^2/\text{s}$ in the a - b plane at 300 K is measured, which is consistent with previous observations.

We are reporting results of high-frequency ($> 1 \text{ GHz}$) optical generation and detection of acoustic waves in the plane of ultrathin ($< 1000 \text{ \AA}$) films. Thin films are of increasing scientific and technological importance. The ability to study acoustic and thermal properties of films, without making mechanical contact can increase our understanding of thin-film materials. Transient gratings¹ have several advantages over more conventional acoustic methods. The grating excites a certain wave vector, which is parallel to the surface, rather than certain frequency. By measuring the frequency of the oscillations seen in the signal, both the wavelength and frequency of the acoustic wave are known. Also, no mechanical contact is made to the sample, avoiding perturbations of the material and influences from acoustic mismatch. Other picosecond-laser acoustic techniques, which use a pump-probe geometry, make use of the echo technique from conventional acoustics.² This generates an acoustic wave packet made up of many modes which travels perpendicular to the surface unlike a transient grating experiment.

The sample in this study is $\text{YBa}_2\text{Cu}_3\text{O}_{7-x}$. This work was initiated to demonstrate the basic aspects of using optical transient grating methods for the study of thin films and to lay the ground work for answering a fundamental question about high-temperature superconductors (HTS), i.e., are these materials BCS superconductors? Since their discovery there have been unsuccessful attempts to perform a temperature dependent acoustic attenuation experiment.³ In a metal, above the superconducting transition temperature, T_c , acoustic waves are damped via electron-gas viscosity. Below T_c , the electron-acoustic phonon scattering is turned off because of electron pairing, and the acoustic attenuation is reduced essentially to zero. The BCS theory predicts a particular form of the acoustic attenuation as the temperature is reduced through T_c .^{4,5} and permits a detailed examination of the superconducting gap.

High quality HTS materials are available as c -axis-oriented thin films (a few hundred to a few thousand Å) on smooth substrates.⁶ Conventional methods for the generation and detection of ultrasonic waves are not readily applicable to thin films or to bulk HTS crystals which are generally very small. These problems, which

have previously prevented detailed acoustic attenuation studies in HTS, can be overcome by applying the picosecond transient grating method.

The experimental system consists of a mode-locked Q -switch Nd:YAG laser which is single pulse selected and doubled to produce a 80-ps pulse at a wavelength of 532 nm and a repetition rate of 1 kHz. The laser beam is split into three beams and attenuated to about $1 \mu\text{J}$ per pulse in each beam. Two of these pulses are time coincident and cross at the MgO - $\text{YBa}_2\text{Cu}_3\text{O}_{7-x}$ interface at an angle θ . Absorption of the optical interference pattern by $\text{YBa}_2\text{Cu}_3\text{O}_{7-x}$ produces electronic excitations that spatially mimic the interference pattern and having a grating wave vector $|\beta| = (2\pi/\text{fringe spacing})$ perpendicular to the surface normal. The Gaussian excitation beams have a $1/e$ diameter of 0.8 mm. The excited electrons rapidly ($\sim 1 \text{ ps}$) relax via electron-phonon coupling⁷ to produce a temperature jump $\approx 0.1 \text{ K}$. The spatially periodic (sinusoidal) temperature profile induces a strain which generates counterpropagating coherent acoustic waves and a nonpropagating thermal pattern.⁸ The combined acoustic wave and thermal pattern form a grating which

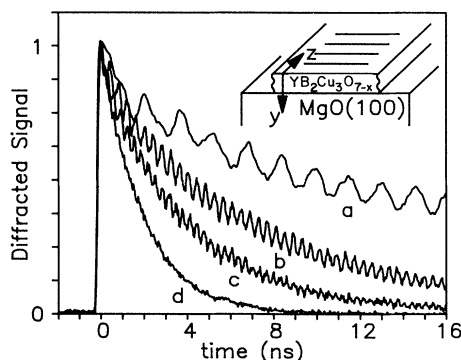


FIG. 1. Transient grating signal from a 350-nm-thick $\text{YBa}_2\text{Cu}_3\text{O}_{7-x}$ film at 300 K for fringe spacings of 8.59, 1.36, 0.94, and $0.68 \mu\text{m}$, corresponding to curves a , b , c , and d , respectively. The inset shows the experimental geometry with the grating peaks indicated by horizontal lines on the $\text{YBa}_2\text{Cu}_3\text{O}_{7-x}$.

is detected by diffracting a third laser pulse from the spatially periodic perturbation of the dielectric constant.⁹

Figure 1 shows data taken at several fringe spacings on a 350-nm-thick $\text{YBa}_2\text{Cu}_3\text{O}_{7-x}$ film at 300 K. The wave vector β is in the z direction ($a-b$ plane, film plane), and y is normal to the $a-b$ plane (c axis of the film). As the fringe spacing becomes smaller the oscillations become faster since the acoustic waves have a wavelength equal to the fringe spacing. The smallest fringe spacing does not show oscillations because the oscillations would be faster than the 80-psec pulse duration used in these experiments.¹⁰ The oscillations are superimposed on the nonexponential decay of a thermal grating.

In a combined acoustic and thermal grating the refractive index changes due to the peak-null density change. The diffraction efficiency $\eta(t)$ is proportional to the square of the grating-peak-null difference in the complex index of refraction. Because the density is not uniform in the y direction, $\eta(t)$ is proportional to the square of the integral over y of the peak-null difference in density,

$$\eta(t) \propto \left[\int_0^b T(y,t) \exp(-\beta^2 D_{a,b} t) - \sum_i A_i(y) \cos(\omega_i t) dy \right]^2.$$

The film-substrate interface and the free surface are at $y=b$ and $y=0$, respectively. $\eta(t)$ has contributions from thermal diffusion and acoustic oscillations. Diffusion in the z direction equalizes the peak-null density and gives rise to an exponentially damped term¹¹ with a decay related to the diffusion constant, $D_{a,b}$. The heat flow in the y direction involves thermal diffusion from the $\text{YBa}_2\text{Cu}_3\text{O}_{7-x}$ into the MgO substrate, which will be discussed below. This contribution to the signal is denoted $T(y,t)$. Counterpropagating acoustic waves of the i th mode produce an oscillation in the peak-null density, and therefore a signal at frequency ω_i .¹ Here, $A_i(y)$ is the

spatial distribution of the i th mode in the y dimension.

To study the effect conduction electrons have on the acoustic damping in thin films, it is necessary to consider the acoustic waveguide nature of the samples. Figure 2 displays three data sets taken on samples with different thicknesses with the Fourier transforms shown in the inset. Two frequencies are clearly present in the 50- and 80-nm-thick samples.

Dispersion curves for the two modes were obtained by performing experiments with a variety of fringe spacings on the three samples. One of the curves is from bulk longitudinal waves in the MgO substrate. The dispersion is a straight line which exactly matches the longitudinal velocity in MgO(100). The generation and detection of this wave will be discussed in detail elsewhere;¹² it is most likely generated by the transient grating Brillouin scattering mechanism⁸ in the bulk MgO.

Figure 3 displays the experimentally determined dispersion curve which corresponds to the first Rayleigh mode¹³ of the system. Frequency values were obtained by taking the Fourier transforms of the data on three samples of different thickness and at five fringe spacings. The dashed lines represent the Rayleigh wave velocity of MgO(100) (upper) and a calculation of the Rayleigh velocity (assuming an isotropic material) of $\text{YBa}_2\text{Cu}_3\text{O}_{7-x}$ (lower).^{14,15} When the wavelength of the mode relative to the thickness of the $\text{YBa}_2\text{Cu}_3\text{O}_{7-x}$ film becomes very large (small βb), a significant portion of the wave resides in the substrate as an evanescent wave. As βb approaches zero, the properties of the mode are dominated by the bulk material constants of the substrate, i.e., the mode becomes a Rayleigh wave of the substrate. Figure 3 shows that the dispersion relation does approach that of MgO in the limit of zero βb . As βb increases, the Rayleigh wave becomes a mode of the film, as indicated by the deviation of the dispersion from the substrate Rayleigh wave velocity and its approach to the $\text{YBa}_2\text{Cu}_3\text{O}_{7-x}$ Rayleigh velocity.

Observation of the temperature dependence of the lowest frequency mode ($\text{YBa}_2\text{Cu}_3\text{O}_{7-x}$ Rayleigh wave) yields the temperature dependence of the acoustic damp-

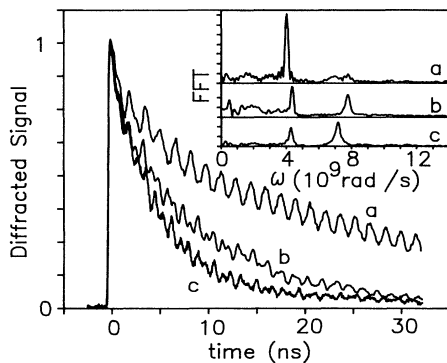


FIG. 2. Transient grating signals for 350-, 80-, and 50-nm-thick $\text{YBa}_2\text{Cu}_3\text{O}_{7-x}$ films correspond to curves *a*, *b*, and *c*, respectively, at 300 K and a fringe spacing of $8.59 \mu\text{m}$. The inset shows faster Fourier transforms (FFT) of the acoustic portion of the data sets. Two frequencies are clearly present in some of the samples.

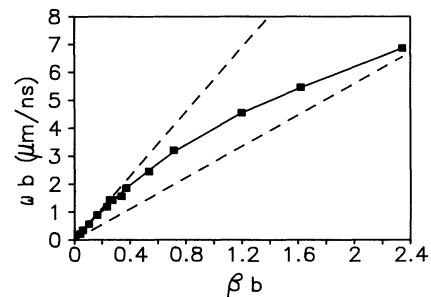


FIG. 3. Acoustic waveguide dispersion curve for the lowest Rayleigh mode of a $\text{YBa}_2\text{Cu}_3\text{O}_{7-x}$ thin film on MgO(100). The dashed lines indicate the Rayleigh wave velocity of MgO(100) (upper line) and $\text{YBa}_2\text{Cu}_3\text{O}_{7-x}$ Rayleigh wave velocity of MgO(100) (upper line) and $\text{YBa}_2\text{Cu}_3\text{O}_{7-x}$ (lower line). A solid line is drawn through the data as a visual aid.

ing and information on the electron-phonon coupling. No appreciable acoustic damping ($\ll 1$ factor of e) is observed over the temperature range of 13 to 300 K in 30 ns for a 1.5-GHz wave. The upper limit for the acoustic damping rate is ~ 100 dB/cm at 1 GHz. In comparison to a conventional superconductor this is very long.^{4,5} One can estimate the acoustic damping in a bulk material. Above T_c , the sound absorption for shear waves is approximately⁴

$$A_s = N \epsilon_F \omega^2 \tau / (5 \rho V_s^3),$$

for $\beta l \ll 1$, where l is the electron mass free path. The carrier density, Fermi energy, shear acoustic velocity, and electron-phonon scattering time are N , ϵ_F , V_s and τ , respectively. For a normal metal,¹⁶ this is $\sim 10^2$ – 10^3 dB/cm at 1 GHz and 10 K. This would be readily observable on the experimental timescale.

The acoustic damping in a $\text{YBa}_2\text{Cu}_3\text{O}_{7-x}$ film is expected to be considerably less than the value for tin for two reasons. First, $\text{YBa}_2\text{Cu}_3\text{O}_{7-x}$ has a substantially lower density of carriers. Second, the waveguide nature of these samples introduces an additional feature. At frequencies (~ 1 GHz) where the wavelength is large compared to the thickness of the films, an evanescent tail extends into the supporting substrate. The MgO substrate has zero damping on the time scale of the experiments. The evanescent wave will not change the temperature dependence of the acoustic damping in the $\text{YBa}_2\text{Cu}_3\text{O}_{7-x}$ film, which is of central importance; however it will reduce the overall magnitude of the damping by a factor of $(b/\text{fringe spacing})^2$.¹⁷ Therefore, by going to significantly higher frequencies, it will be possible to observe the temperature dependence of the acoustic damping. The high-frequency experiments are currently in progress.

Heat flow in the $a-b$ plane was studied by varying β from 0.68 to 8.59 μm on three films (see Fig. 1). Since $T(y,t)$ is independent of β , plotting the inverse of the long-time exponential decay varies β^2 should yield a straight line with a slope equal to $D_{a,b}$. This behavior is observed in Fig. 3. The measured diffusion constant is independent of sample thickness. The individual slopes are given in Table I with an average value of 0.023 cm^2/s . This yields a thermal conductivity of 4.8 $\text{Wm}^{-1}\text{K}^{-1}$, which coincides with the literature value of 4.8 ± 0.1 $\text{Wm}^{-1}\text{K}^{-1}$.¹⁸

For heat flow in the direction parallel to the c axis (y

direction) the diffusion equation is solved with the appropriate boundary conditions. On the free boundary at $y=0$, no heat flows out of the sample, i.e., $dT/dy=0$. The thermal conductivity of MgO (100 $\text{Wm}^{-1}\text{K}^{-1}$) is about 2 orders of magnitude higher than for $\text{YBa}_2\text{Cu}_3\text{O}_{7-x}$, and the boundary condition which assumes an infinitely fast flow across the MgO/ $\text{YBa}_2\text{Cu}_3\text{O}_{7-x}$ interface is $T=0|_{y=b}$. For barrier-limited thermal diffusion, the boundary condition is

$$D_y dT/dy|_{y=b} = D^* T/\delta|_{y=b},$$

where D^* and δ are the thermal diffusivity and thickness of the barrier, respectively. Solving the diffusion equation with these boundary conditions in the long-time limit¹⁹ yields the longest exponential decay time in the diffracted signal,

$$\tau_0 = 4b^2/D_y \pi^2,$$

if there is no barrier to diffusion. If there is a significant barrier, the longest decay time is

$$\tau_0^* = \delta b/D^*.$$

The important feature of these two cases in their distinct dependences on sample thickness. If heat flow into the substrate is limited by a barrier the decay is proportional to b ; if not it is proportional to b^2 .

In the limit that the fringe spacing becomes infinite, thermal diffusion in the $a-b$ plane drops out of the signal time dependence. The y intercepts in Fig. 4 are experimental determinations of the longest exponential decay time (τ_0 or τ_0^*) of the heat flow into the MgO substrate. The values of these intercepts ($\beta^2=0$), $\tau(0)$, are given in row 2 of Table I. Row 3 of Table I clearly shows that the linear functional form gives a nearly constant value while row 4 shows that the quadratic form is far from constant. Therefore, the flow of heat into the MgO is limited by a barrier at the $\text{YBa}_2\text{Cu}_3\text{O}_{7-x}$ /MgO interface. If the barrier is assumed to be 10 \AA wide, the

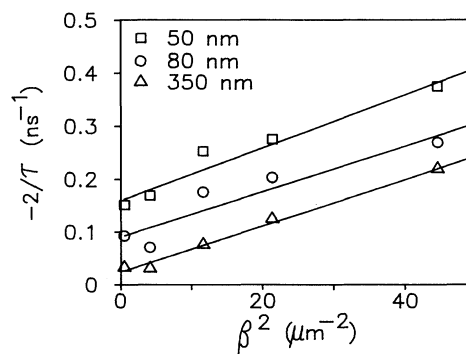


FIG. 4. Grating wave vector (β) dependence of the longest time component (τ_0) of the heat flow for three $\text{YBa}_2\text{Cu}_3\text{O}_{7-x}$ films of thicknesses 50, 80, and 350 nm at 300 K. The thermal diffusivity in the $a-b$ plane, 0.023 cm^2/s , is given by the average slope.

TABLE I. Diffusion constant, $D_{a,b}$ and transient grating decay parameters for $\text{YBa}_2\text{Cu}_3\text{O}_{7-x}$ films of three different thicknesses.

	Thickness b (nm)		
	350	80	50
$D_{a,b}$ (cm^2/s)	0.022	0.022	0.025
$\tau(0)$ (ns)	83	22	12.5
$b/\tau(0)$ (nm/ns)	4.2	3.6	4.0
$b^2/\tau(0)$ (nm^2/ns)	1500	290	20

thermal diffusivity in the c direction across the interface can be estimated to be $4 \times 10^{-5} \text{ cm}^2/\text{s}$. This is more than 2 orders of magnitude slower than the diffusivity in the a - b plane of $\text{YBa}_2\text{Cu}_3\text{O}_{7-x}$.

In conclusion, we have demonstrated a method capable of giving detailed information on acoustic wave propagation in the plane of thin films ($\sim 1000 \text{ \AA}$). The demonstration of the applicability of this method should now make it possible to study temperature dependent acoustic damping of high-temperature superconductors. To perform the damping experiments it is necessary to increase either the acoustic frequency or the laser spot size with longer delay times. Both approaches are practical. The only ultimate limitation of the transient grating sensitivity for acoustic damping is the sample width. In general,

the transient grating technique also provides insight into heat flow in thin films, and the experiments show that heat flow from $\text{YBa}_2\text{Cu}_3\text{O}_{7-x}$ into the MgO substrate is barrier limited.

We would like to thank Professor T. H. Geballe and C. B. Eom for many informative discussions and for providing the outstanding quality samples necessary for these experiments. We would also like to thank Dr. Li Song for his assistance with the experimental apparatus, and S. R. Greenfield for his assistance with computer programming. This work was supported by the National Science Foundation, Division of Materials Research (DMR87-18959). One of the authors (I.M.F.) acknowledges ONR (N00014-86-K-0118) for partial support.

*Also at W. W. Hansen Experimental Physics Laboratory, Stanford University, Stanford, California 94305.

- ¹J. S. Meth, C. D. Marshall, and M. D. Fayer, *J. Appl. Phys.* **67**, 3323 (1990).
- ²H. T. Grahn, H. J. Maris and J. Tauc, *IEEE J. Quantum Electron.* **25**, 2562 (1989), and references therein.
- ³K. J. Sun, W. F. Winfree, M-F. Xu, M. Levy, B. K. Sarma, A. K. Singh, M. S. Osofsky, V. M. Le Tourneau, *Physica C* **162-164**, 446 (1989).
- ⁴W. P. Mason, *Physical Acoustics and the Properties of Solids* (Nostrand, Princeton, 1958), Chap. 11.
- ⁵R. Morse, H. Bohm, *Phys. Rev.* **108**, 1094 (1957).
- ⁶C. B. Eom, J. Z. Sun, K. Yamamoto, A. F. Marshall, K. E. Luther, T. H. Geballe, and S. S. Landerman, *Appl. Phys. Lett.* **55**, 595 (1989).
- ⁷S. D. Borson, A. Kazeroonian, J. S. Moodera, D. W. Face, T. K. Cheng, E. P. Ippen, M. S. Dresselhaus, G. Dresselhaus, *Phys. Rev. Lett.* **64**, 2172 (1990).
- ⁸M. D. Fayer, *IEEE J. Q. Elec.* **22**, 1437 (1986).
- ⁹K. A. Nelson, R. Casalegno, R. J. D. Miller, and M. D. Fayer, *J. Chem. Phys.* **77**, 1144 (1982).
- ¹⁰L. Genberg, Q. Bao, S. Gracewski, and R. J. D. Miller, *Chem. Phys.* **131**, 81 (1989).
- ¹¹V. J. Newell, T. S. Rose, and M. D. Fayer, *Phys. Rev. B* **32**, 8035 (1985).
- ¹²I. M. Fishman, C. D. Marshall, and M. D. Fayer (unpublished).
- ¹³B. A. Auld, *Acoustic Fields and Waves in Solids* (Wiley, New York, 1973), Vol. 2, Chap. 10.
- ¹⁴G. W. Farnell and E. L. Adler, in *Physical Acoustics*, edited by W. P. Mason and R. N. Thurston (Academic, New York, 1972), Vol. 9, Chap. 2.
- ¹⁵M. H. Ledbetter, in *Proceedings of the MRS International Meeting on Advanced Materials* (MRS, Pittsburgh, 1989), Vol. 6, p. 689.
- ¹⁶W. P. Mason, *Phys. Rev.* **97**, 557 (1955).
- ¹⁷S. C. Schneider, *IEEE Trans. Ultrason. Ferroelectrics Frequency Control*, **36**, 114 (1989), and references therein.
- ¹⁸A. Jezowski, K. Rogacki, R. Horyn, and J. Klamut, *Physica C* **153-155**, 1347 (1988).
- ¹⁹P. R. Wallace, *Mathematical Analysis of Physical Problems* (Dover, New York, 1984).